ADVANCED OPTICAL MATERIALS
www.advopticalmat.de

Fabrication of Plastic Optics from Chalcogenide Hybrid Inorganic/Organic Polymers for Infrared Thermal Imaging

Jake Molineux, Taeheon Lee, Kyung Jo Kim, Kyung-Seok Kang, Nicholas P. Lyons, Abhinav Nishant, Tristan S. Kleine, Sam W. Durfee, Jeffrey Pyun, and Robert A. Norwood*

The development of infrared (IR) plastic optics for infrared thermal imaging, particularly, in the long-wave IR (LWIR) spectrum (7–14 µm) is an area of growing technological interest due to the potential advantages associated with plastic optics (e.g., moldability and low cost). The development of a new class of optical polymers, chalcogenide-based inorganic/organic hybrid polymers (CHIPs) derived from the inverse vulcanization of elemental sulfur, has enabled significant improvements in IR transparency due to reduction of IR absorbing organic comonomer units. The vast majority of effort has focused on new chalcogenide hybrid polymer synthesis and optical property improvements (e.g., refractive index, Abbe number, and LWIR transmission); however, fabrication and IR imaging methodology to prepare optical components has not been demonstrated, which remains critical to develop viable IR plastic optics. A new methodology is reported to fabricate optical components and evaluate LWIR imaging performance of this emerging class of optical polymers. New diffractive flat optics with a Fresnel lens design for these materials have been developed, along with a basic LWIR imaging system to evaluate CHIPs for LWIR imaging. This system-based approach enables correspondence of copolymer structure-property correlations with LWIR imaging performance, along with demonstration of room temperature LWIR imaging.

1. Introduction

The use of infrared thermal imaging for consumer electronics, security, aerospace, automotive, and housing markets has demonstrated the benefits of this technology beyond use in the defense sector.[1] IR thermal imaging can be conducted in the midwave (3–5 µm) and long wave (7–14 µm) spectrum and is primarily based on detecting black body radiation emitted by imaging targets at these respective wavelengths. The wider deployment of IR thermal imaging systems has been stifled by the high cost associated with the IR cameras and electronics, which is particularly an issue for mid-wave infrared (MWIR) and long-wave infrared (LWIR) imaging systems that use semiconductor photodetectors that require low-temperature refrigeration to suppress background dark current due to the low bandgap of the detectors.[2] LWIR imaging systems can be significantly less expensive with the use of (micro)bolometer sensors based on materials with large temperature-dependent resistance (e.g., vanadium oxide), however, the trade-off is reduced sensitivity versus mercury cadium telluride ($Hg_xCd_{1-x}Te$) or other semiconductor LWIR photodetection.[1–3] Nevertheless, a significant expense for LWIR imaging systems is for transmissive optical elements (e.g., lenses, windows) based on costly materials, such as, germaniuam (Ge) or chalcogenide glasses (ChG's).[1,2]

While plastic optics have been highly desirable for use as LWIR transmissive materials due to the low cost and manfacturability of synthetic plastics (via molding-casting), organic materials are instricially poor for IR optics due to strong MWIR and LWIR absorption from carbon atom-based bond vibrational modes. One notable exception is polyethylene, where the chemical simplicity of this material (e.g., only sp^3 C–C, C–H bonds) affords sharp degenerate vibrational peaks outside of the commonly used LWIR spectrum (8–12 µm). In the case of Ge, or ChG materials, the much higher mass of the vibrating atoms (e.g., Ge-Ge) results in very low frequency vibrations compared to those commonly encountered in polymers (e.g., C–H, C–C, C–O, C-X bonds) and hence, these materials do not absorb in the LWIR spectral window.[2,4]

A significant advance in the field of optical polymeric materials was the discovery of *Chalcogenide Hybrid Inorganic/Organic Polymers (CHIPs)* by Pyun and Norwood et al.[5] (this class of sulfur copolymers is also referred to as inverse vulcanized polymers,[6] or organically modified chalcogenides[7] in subsequent reports) which are a recently developed class of polymers possessing high refractive index values (n = 1.7 to 2.1 in the near IR) and improved optical transparency across portions of the visible and infrared wavelengths.[2,5] These materials are prepared by the

J. Molineux, T. Lee, K.-S. Kang, T. S. Kleine, S. W. Durfee, J. Pyun
Department of Chemistry and Biochemistry
University of Arizona
Tucson, AZ 85721, USA
E-mail: jpyun@email.arizona.edu
K. J. Kim, N. P. Lyons, A. Nishant, J. Pyun, R. A. Norwood
J. C. Wyant College of Optical Sciences
University of Arizona
Tucson, AZ 85721, USA

The ORCID identification number(s) for the author(s) of this article can be found under https://doi.org/10.1002/adom.202301971

DOI: 10.1002/adom.202301971

direct copolymerization of organic saturated comonomers with elemental sulfur (S_8) (and selenium) via a process termed, *inverse vulcanization*.[8] The unusually high content of S–S bonds in the polymeric backbone imparts both high refractive index (RI) values, but also unprecedented optical transparency for synthetic polymers in the infrared spectrum due to the reduced organic content in the material and the shifted absorbances of S–S bonds outside of the MWIR and LWIR spectral windows used for thermal imaging.[2] Recent efforts by numerous groups have focused on design of organic comonomers in the inverse vulcanization process to enhance the LWIR transparency of high sulfur content polymers derived from S_8 and the inverse vulcanization process, which now include, tetravinyltin,[7b] dimeric norbornadiene (NBD2),[5e] aryl halides,[9] benzene-1,3,5-trithiol,[10] 1,3,5-trivinylbenzene[11] and cyclopentadiene.[12] However, an intrinsic limitation with S_8-derived *CHIPs* is the requisite organic comonomer phase (typically 10–50 wt.% in the material), which ultimately limits LWIR transparency relative to Ge, or ChG's.

To date, the fabrication of refractive optics with *CHIPs* has not been conducted for IR thermal imaging, with early-stage efforts focused on the development of melt processing methods to form freestanding flat windows, or replicas of non-specific elements for both MWIR and LWIR imaging experiments. However, the full design, fabrication, and successful imaging of *CHIPs*-based plastic optics for LWIR thermal imaging has not to date been conducted. Related efforts on the solution processing of one-dimensional photonic crystals[13] and photolithographic fabrication of photonic devices (waveguides, splitters, ring-resonators) with *CHIPs* have been demonstrated.[14] Furthermore, *CHIPs* MWIR polarizers were fabricated into thin film components by Wie et al.[15] via melt-processing using nanoimprint lithographic methods. Recent efforts to fabricate LWIR plastic optics have focused on the development of flat diffractive optics using PMMA,[16] or hybrid polymer-silicon-based materials,[17] which can then be prepared as thin film optical lenses (thicknesses << 100 microns) to mitigate the poor LWIR transparency of these organic polymers. Flat diffractive optics include Fresnel lenses[18] and more complex metalens systems,[19] which require lithographic fabrication of micro-structured features for optical phase control; due to the very large refractive index contrast required for metalenses, Fresnel lenses are an excellent choice for implementing successful IR plastic optic fabrication for many applications. Polyethylene (PE) based Fresnel lenses for LWIR imaging have been commercialized and are currently the only viable polymeric LWIR plastic optic.[20] However, PE has significant limitations as an IR transmissive material, which include limited processability for optical fabrication (PE cannot be cast, thus PE Fresnel lenses require diamond turning fabrication which raises cost), high crystallinity which leads to reduced transmission from light scattering, and low refractive index. Hence, there remains a need for the development of novel synthetic amorphous polymeric materials and optical fabrication methods for *CHIPs* for IR optical elements to open new possibilities for LWIR plastic optics.

Herein, we report on the first successful fabrication of *CHIPs* plastic optics based on Fresnel lenses and the demonstration of LWIR thermal imaging. The current report discusses numerous advances on the fabrication methods for LWIR plastic optics, along with the development of an inexpensive prototype imaging system using a commercially available microbolometer LWIR detector. Furthermore, we report on the development of low-cost IR imaging resolution targets based on laser stenciled PMMA sheets to standardize LWIR imaging experiments,[5e] which have historically relied on empirical IR thermal imaging of human specimens, or other ambient environment targets. *CHIPs* based on poly(sulfur-*random*-dimeric norbornadiene) (poly(S-*r*-NBD2)[5e] was readily suited for fabrication of LWIR plastic optics, due to the melt-processability and moldabilty of this polymeric material, along with favorable thermomechanical properties that suppressed reflow of molded optical components, all of which were essential to fabricate IR plastic optics capable of LWIR imaging.

2. Results And Discussion

The key barriers to validation of *CHIPs* as transmissive optical materials for LWIR imaging can be summarized into the following efforts: 1) fabrication of functional refractive optical lenses; 2) fabrication of LWIR imaging resolution targets to standardize imaging across new system; and 3) integration of the fabricated lenses and resolution targets into a simple, inexpensive LWIR imaging system to enable uniform standardization and evaluation of imaging experiments.

2.1. Materials Considerations and Fresnel Lens Fabrication

In the fabrication of plastic optics, it is the ensemble of cost, optical/thermomechanical properties, and polymer processibility that determine suitability for final end-use as LWIR transmissive optical components. While high chalcogenide content compositions were presumed to be better suited for LWIR plastic optics due to improved LWIR transmission of S-S bonds, high sulfur content compositions may also compromise thermomechanical integrity and processibility of optical lenses, resulting in increased light scattering. Hence, poly(S-*r*-NBD2) with 50 wt.% and 70 wt.% sulfur were chosen for Fresnel lens fabrication and imaging as these copolymers possessed the overall best combination of LWIR %T, glass transition (T_g)/thermal stability and melt processability, as determined previously through flat window fabrication and optical characterization (**Figure 1**a,c,d). First-generation *CHIPs* based on poly(sulfur-*random*-(1,3-diisopropenylbenzene)) ((poly(S-*r*-DIB), Figure 1b) copolymers[5a,8a] at the same composition (50 wt.%, 70 wt.%) were used to prepare reference lenses to highlight the superior properties of poly(S-*r*-NBD2) due to the observed inferior IR transparency and thermomechanical properties of poly(S-*r*-DIB). Low T_g polymers such as poly(S-*r*-DIB) (T_g < 40 °C)[5a,8a] are subject to reflow after initial molding into optical elements, which can result in lens distortion with time or at elevated temperatures as discussed in later sections. General designations for sulfur copolymers with varying sulfur wt.% compositions are noted by subscripts inserted into the polymer abbreviations (e.g., poly(S_{50}-*r*-$NBD2_{50}$) and poly(S_{70}-*r*-$NBD2_{30}$) for 50-wt% and 70-wt% sulfur). IR spectroscopy of poly(S_{50}-$NBD2_{50}$) free-standing films of varying thickness (0.1 mm (1), 0.7 mm (2), and 1.0 mm (3), Figure 1c) was conducted to extrapolate the LWIR transmittance of fabricated Fresnel lenses, which confirms good optimal transmittance in the 0.1 mm thickness range, with a significant reduction in LWIR transmission above this thickness regime. Hence, this confirmed that supported thin poly(S-*r*-NBD2) Fresnel lenses in this thickness regime would be viable

ADVANCED OPTICAL MATERIALS
www.advopticalmat.de

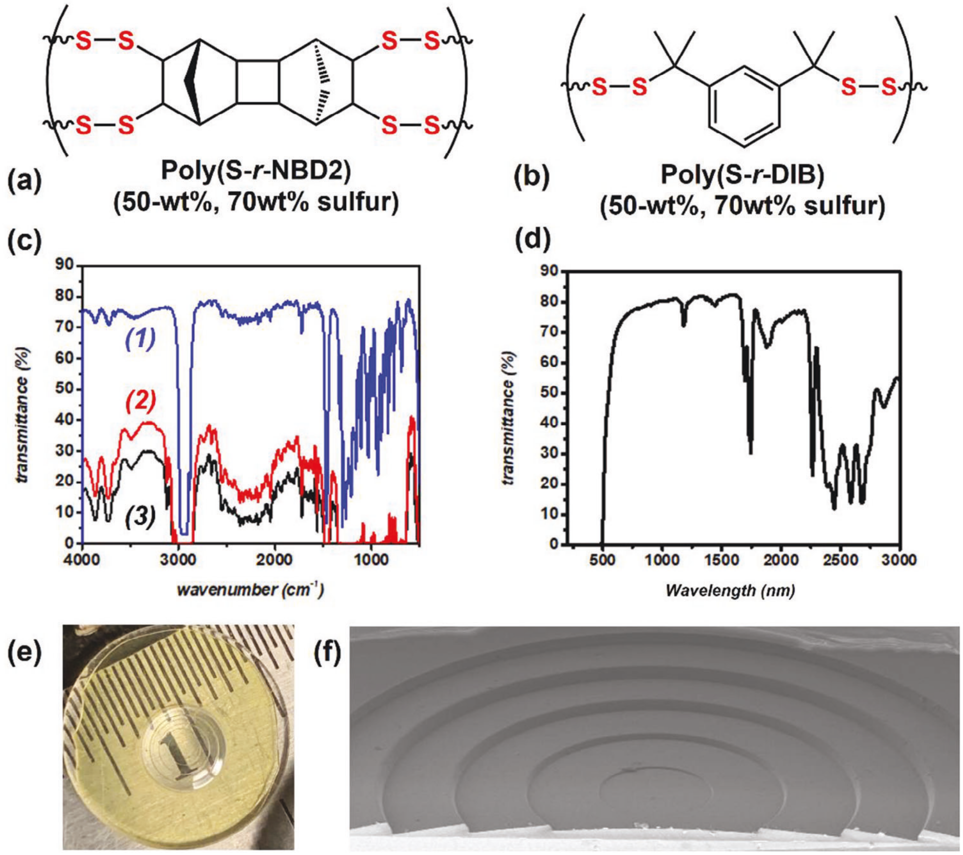

Figure 1. Chemical structures of optical *CHIPs* materials used for Fresnel lens fabrication a) poly(S-*r*-NBD2) and b) poly(S-*r*-DIB) with either 50 wt.% or 70 wt.% sulfur; c) IR spectrum of 1.0 mm (3), 0.7 mm (2), and 0.1 mm (1) thick films of poly(S_{50}-r-$NBD2_{50}$) with 50 wt.% sulfur; d) Vis-NIR-SWIR transmission spectrum of 1.0 mm thick film of poly(S_{50}-*r*-$NBD2_{50}$) with 50 wt.% sulfur; e) poly(S_{50}-*r*-$NBD2_{50}$) thin film Fresnel lens (0.1 mm, thick) cast onto a NaCl plate; and f) SEM image at 20° tilt of (e).

candidates for LWIR imaging under ambient conditions. An additional advantage of poly(S-r-NBD2) materials for IR plastic optics versus inorganic materials, such as, germanium, is the high optimal transmittance of this sulfur copolymer in many regions of the Vis-NIR-SWIR spectrum (see Figure 1d for representative transmission spectrum of 1.0 mm thick poly(S_{50}-*r*-DIB_{50}) film). This is a notable advantage for systems fabrication as optical alignment can be conducted at VIS-NIR wavelengths which it not possible in semiconductors (e.g., Si, Ge) that are opaque in the visible spectral region.

Before designing the appropriate Fresnel lens for use in IR imaging, the selection of a suitable LWIR detector was necessary. The FLIR Lepton 2.5 was selected as it is a commercially available, low-cost system that also comes with signal processing electronics and software to enable quantitative temperature mapping. The pixel size of the Lepton was 12 µm with a focal plane area of ≈0.5 mm,[2] and the refractive index of poly(S-*r*-NBD2) was assumed to be 1.8, approximately appropriate for both the 50 wt.% and 70 wt.% sulfur compositions. With these general detector specifications in mind, Fresnel lens design for the poly(S_{50}-r-$NBD2_{50}$) material was then conducted. When designing a lens, properties such as the *f-number* (F/#), field of view, detector size, and pixel size need to be considered.[21] It is also critical to minimize aberrations to ensure the highest imaging quality. However, for imaging applications using Fresnel lenses, there are additional factors that need to be considered. For example, to maximize imaging quality, the profile of the lens will include a conic constant in the lens profile. Since the process of diamond turning, which was used to make the mold master, does not become much more expensive as the complexity of the lens profile increases, a conic constant was added to the curved lens profile to improve resolution. In order to reduce diffraction effects and optimize image quality, the number of Fresnel zones was kept low. This Fresnel spacing was set to be 0.5 mm between zones [100], with a total of 5 zones for an entrance pupil diameter of 5 mm. The optical ray tracing software CODE V was used to realize an approximately diffraction-limited design on-axis with a 10 mm focal length.

To enable melt polymer processing via casting of *CHIPs* materials, the Fresnel lens master was fabricated via diamond turning into a flat PMMA window (≈4 mm thickness; 2 cm diameter) followed by preparation of a soft PDMS mold from the PMMA master (see Experimental section for details). Sulfur copolymer Fresnel lenses made from NBD2 or DIB were made by pouring low viscosity/mid-conversion bulk inverse vulcanization reactants into the PDMS molds and curing at $T = 165$ °C for one hour. This process either enabled thin films (≈100 micron thickness, Figures 1e,f and 3b–d) of sulfur copolymer Fresnel lenses

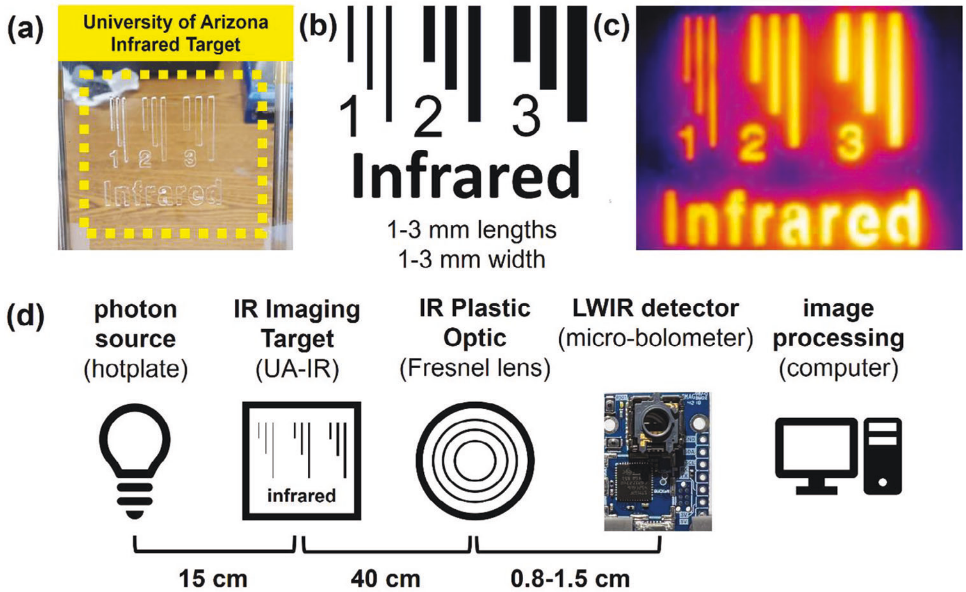

Figure 2. a) UA-IR target fabricated for LWIR imaging standardization prepared from CO_2 laser writing into PMMA sheet; b) specifications of UA-IR target pattern, with each line ranging from 1 to 3 mm in length and width; c) representative LWIR image of UA-IR target; and d) schematic of labscale prototype LWIR imaging system.

for casting onto LWIR transparent NaCl supporting substrates or freestanding Fresnel lenses (thickness = 0.7 or 1 mm, Figure 4) with successful replication of the PMMA Fresnel lens master as readily visualized by SEM imaging (Figure 1f).

2.2. LWIR System Assembly and Imaging Standardization

Access to both IR plastic optics lens fabrication methods AND creation of a low-cost complete LWIR imaging system remain key technological limitations for new LWIR optical polymer development. With access to both substrate-supported and freestanding *CHIPs* Fresnel lenses, integration into a functional LWIR imaging system was the next step required to evaluate the optical performance of the fabricated lenses and candidate optical polymers for LWIR transmissive optical elements (**Figure 2**).

As discussed previously, the LWIR detector chosen for this labscale system was the FLIR Lepton 2.5 microbolometer, with acceptable LWIR detector sensitivity from 8–14 µm. With access to *CHIPs* Fresnel lenses and plano-convex Ge lenses possessing focal lengths of 15 mm, the entire LWIR system could be mounted on an air table, or even on laboratory bench tops, where laboratory scale hotplate-stirrers (or other blackbody radiators) could be used as an inexpensive IR photon source (Figure 2d). To date, there still is no clear LWIR imaging protocol, or resolution targets to enable quantitative, uniform standardization of imaging experiments and new optical element optical characterization, as new LWIR imaging demonstrations are done with highly variable human subjects, or other macroscopic, commonplace tools, or objects (e.g., soldering irons, heating coils). For new optical imaging systems designed for the visible, near-IR, or SWIR spectrum, the use of the **1951 United States Airforce Resolution Test chart (**i.e., USAF target) is now common practice, where the USAF Target is fabricated onto a glass slide (≈2 inches diameter per side) with an assortment of shapes and numbers of varying size and spacing to enable the evaluation of magnification and resolution ranges for new optical imaging systems. To enable facile, but uniform evaluation of LWIR imaging experiments, we further developed on our concept of using PMMA imaging targets made by carbon dioxide laser stencil writing into plastic sheets.[5e] We designed a simple target pattern fabricated by CO_2 laser writing into a PMMA sheet of hollow lines and numbers varying from 1 to 3 mm in length and width and the word, *Infrared*, which when placed in front of a blackbody radiator, would create a well-defined optical resolution test chart, which we now refer to as the University of Arizona Infrared Target (UA-IR target) (Figure 2a–c). The standard USAF target cannot be used for LWIR experiments since the glass substrate is highly absorbing in the LWIR.

2.3. LWIR Imaging Experiments with CHIPs Plastic Optics

With the lens fabrication process and LWIR imaging systems in hand, LWIR imaging experiments comparing Ge and *CHIPs* plastic optics were conducted. To establish a visual benchmark for these new IR thermal imaging results, LWIR experiments were initially conducted with a commercially available plano-convex singlet Ge lens (15 mm focal length, 5 mm thickness, with antireflective (AR) coating) from 100 to 30 °C (**Figure 3**a), where sharp resolution of the UA-IR target was observed as expected across this full temperature range, with progressively reduced image brightness at lower temperatures due to lower IR photon flux generated from the blackbody radiator shown in Figure 2. It is important to note here that the AR-coating on the Ge lens significantly raised the LWIR transmission versus an uncoated Ge lens (LWIR $\%T_{with\ AR} > 90\%T$; LWIR $\%T_{without\ AR} > 50\%T$, see

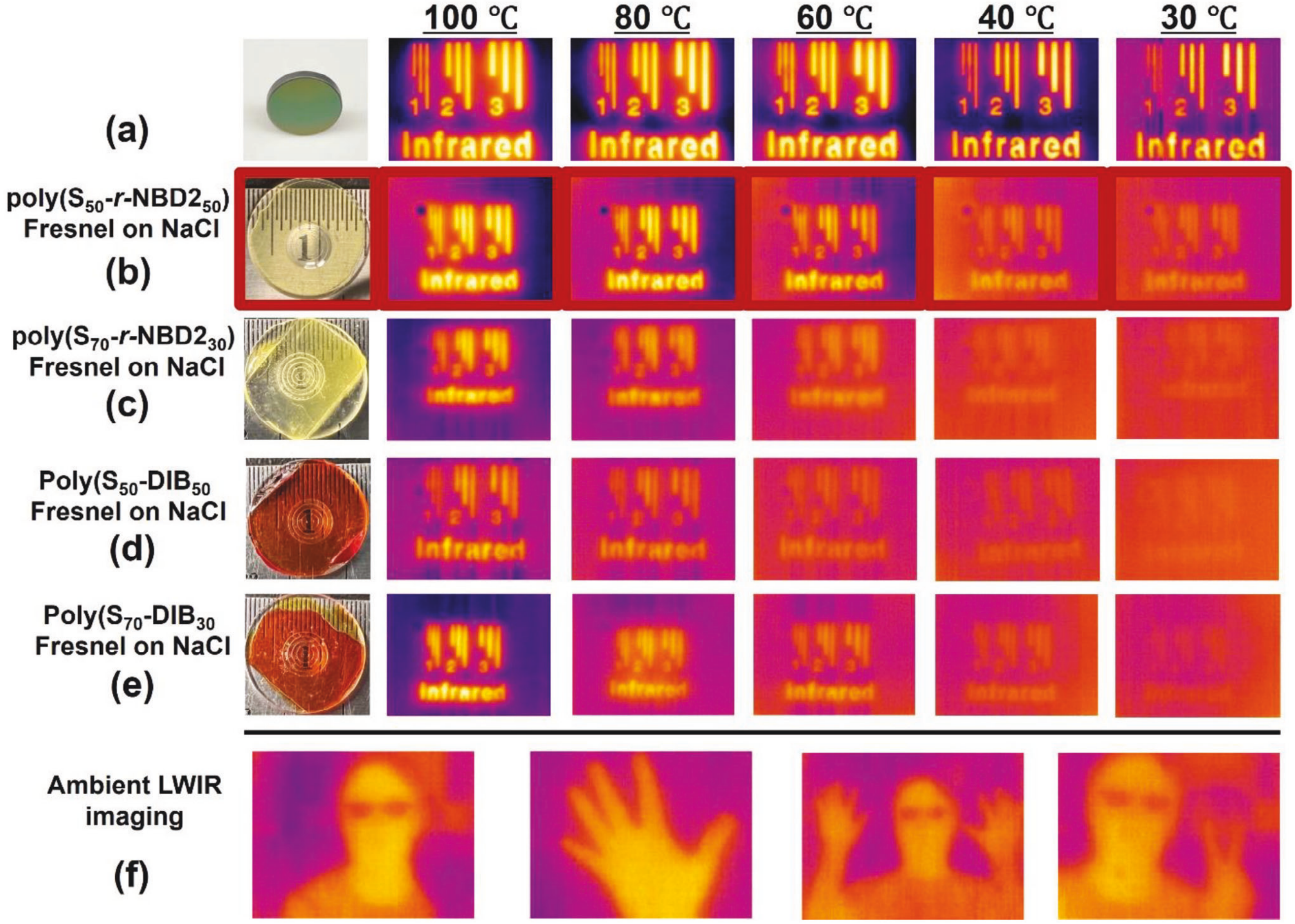

Figure 3. Masked LWIR imaging experiments conducted with UA-IR target and labscale imaging system from Figure 2 from $T = 100$–30 °C for: a) 15 mm focal length plano-convex Ge lens as an imaging reference; b) poly(S_{50}-*r*-NBD2_{50}); c) poly(S_{70}-*r*-NBD2_{30}) thin film Fresnel lens on NaCl; d) poly(S_{50}-*r*-DIB$_{50}$); and e) poly(S_{70}-*r*-DIB$_{30}$) thin film Fresnel lens on NaCl. LWIR imaging was viable for poly(S_{50}-*r*-NBD2_{50}) Fresnel lens from $T = 100$–30 °C, while the control poly(S-*r*-DIB) Fresnel lenses possess inferior intrinsic LWIR transparency and was limited to imaging temperatures above $T = 60$ °C. f) LWIR imaging under ambient conditions with a human subject with NaCl supported poly(S_{50}-*r*-NBD2_{50}) thin film Fresnel lens.

Supporting Information, Figure S1) and afforded higher resolution imaging at low temperatures. Conversely,

LWIR imaging experiments done in the absence of the Ge lens were confirmed to be completely defocused across this temperature range, validating both the LWIR prototype system design, and imaging conditions. The desired LWIR imaging performance with *CHIPs* Fresnel lenses is to achieve high resolution of the UA-IR target down to ambient temperature conditions.

LWIR imaging of poly(S_{50}-*r*-NBD2_{50}) materials was initially done with supported thin film Fresnel lenses (peak thickness ≈100 µm) cast onto NaCl substrates through the UA-IR PMMA target to ascertain both the true LWIR imaging quality and viable thermal imaging ranges of the intrinsic polymer material. The large form factor and limited manufacturabilty of NaCl plates limits direct integration of this lens architecture into LWIR imaging systems, as will be discussed in later sections. LWIR imaging over 100–30 °C was conducted (Figure 3b), where excellent resolution and brightness was observed with the poly(S_{50}-*r*-NBD2_{50}) Fresnel lens from $T = 100$–60 °C. However, good resolution of the UA-IR target could still be achieved at $T = 40$–30 °C for only this particular Fresnel lens, with an accompanying reduction in image brightness, as observed for the AR-coated Ge lens reference. LWIR imaging with the higher sulfur content poly(S_{70}-*r*-NBD2_{30}) Fresnel lens was anticipated to afford better LWIR imaging and lower temperatures versus the 50 wt.% copolymer experiments, due to the reduced content of organic LWIR absorbing phase. While imaging of the UA-IR target is discernable from $T = 100$–60 °C with image blurring of the target at $T = 40$-30 °C (Figure 3c), it is clear that these LWIR images have poor contrast in comparison to the results from the poly(S_{50}-*r*-NBD2_{50}) lens. This particular effect of LWIR imaging quality on sulfur copolymer compositions points to issues in the fabrication and quality of Fresnel lenses. The poly(S_{70}-*r*-NBD2_{30}), has both slightly lower T_g and more residual unreacted S_8 in the glassy matrix of the lens, both of which may compromise the Fresnel lens quality (e.g., flatness, diffractive pattern resolution), increase scattering losses and present more challenges in optimizing the casting step into PDMS molds. Hence, the superior LWIR imaging quality achieved with the poly(S_{50}-*r*-NBD2_{50}) Fresnel lens reinforces the importance of both materials properties (optical, thermomechanical) and processability (castability, consumption of S_8 solid monomer) to achieve optimal imaging performance.

LWIR imaging experiments with poly(S-*r*-DIB) Fresnel lenses of identical thickness supported on NaCl plates exhibited significantly smaller temperature ranges (T = 100–60 °C), where a significant reduction of LWIR imaging quality was observed below T = 60 ° C for both 50 wt.% and 70 wt.% compositions (Figure 3d,e). The reduced LWIR transmission of poly(S-*r*-DIB) versus poly(S-*r*-NBD2) is the most likely cause of poor LWIR imaging contrast in these experiments, although contributions from inferior thermomechanical properties and processability cannot be ruled out in this thin film NaCl supported lens architecture.

With a series of fabricated IR Fresnel lenses and imaging results in hand, assessment of image resolution and brightness can be directly compared to ascertain which sulfur copolymer compositions afford the highest quality LWIR imaging results. Given the novelty of synthetic plastics, such as *CHIPs*, for LWIR plastic optics, this series of fabrication and imaging experiments, while qualitative in nature, are an important milestone toward creation of viable LWIR lenses and imaging systems. A gross survey of these experiments confirmed that the highest contrast imaging is achieved with the poly(S_{50}-*r*-$NBD2_{50}$) Fresnel lens with the poly(S_{70}-*r*-$NBD2_{30}$), poly(S_{50}-*r*-DIB_{50}) and poly(S_{70}-*r*-DIB_{30}) all exhibiting comparable levels of inferior imaging temperature ranges and resolution. We can estimate image resolution the poly(S_{50}-r-$NBD2_{50}$) Fresnel lens experiments in object space, as resolution of 1 mm thick lines in the UA-IR target can be quoted as an object space resolution of 0.5 cycles mm^{-1} (since one cycle of lines is 2 mm). The image plane resolution can determined by counting the number of pixels from the dark point of the 1 mm line to the next dark or light side feature in the target from the LWIR images from the poly(S_{50}-r-$NBD2_{50}$) Fresnel lens. This corresponds to about 6 pixels in the microbolometer image plane, so one cycle is 6 × 12 = 72 µm, giving an approximate image space spatial frequency resolution of 14 cycles mm^{-1}.

The viability of the poly(S_{50}-*r*-$NBD2_{50}$) thin film Fresnel lenses to achieve masked LWIR imaging of the UA-IR target at T = 40 °C and 30 °C pointed to the likelihood of direct LWIR imaging of black body radiator subjects under ambient conditions. Hence, direct black body LWIR imaging of human subjects was conducted under ambient conditions with NaCl supported poly(S_{50}-*r*-$NBD2_{50}$) thin film Fresnel lens, where the ability to resolve single human subject targets (e.g., face-head, hands-fingers) and multiple component targets (i.e., human subject head & hand, head/hand/fingers) was demonstrated (Figure 3f). While these ambient LWIR images exhibit reduced feature sharpness and resolution, nevertheless, these results demonstrate the viability of room temperature LWIR imaging. This is the first example of *in operando* imaging under ambient conditions with a refractive *CHIPs* plastic lens specifically designed for a LWIR imaging system. Furthermore, the ensemble of lens material and temperature variations point to the validity of this low-cost, standard experimental approach developed for plastic optic fabrication, optical characterization and imaging. Chalker et al. have notably demonstrated the ability to mold a *CHIPs* Frensel lens of appreciable thickness (≈1 mm) and achieve non-refractive LWIR imaging under ambient conditions in conjunction with a commercial LWIR camera.[12] Similar non-refractive LWIR imaging through a molded flat window (thickness ≈1 mm) from *CHIPs* was also achieved by Lee et al. under ambient conditions with the aid of a LWIR camera.[10]

Despite the success of thin film-supported poly(S-*r*-NBD2) Fresnel lenses, the fabrication of *CHIPs* plastic optics into more manufacturable lens formats was also investigated. These efforts included replacing NaCl salt plates with silicon wafer supporting substrates, however, with the aim of large-scale molding of inexpensive LWIR plastic optics, we deemed that fabrication of free-standing, all plastic *CHIPs* Fresnel lenses the more important demonstration to benchmark the bulk material optical performance for LWIR imaging. Freestanding poly(S_{50}-*r*-$NBD2_{50}$) Fresnel lens were cast using the same molding methods previously discussed, except to a total thickness of 1 mm for the final molded optical element. Due to the thermomechanical robustness of poly(S_{50}-*r*-$NBD2_{50}$) material and molded lens, thinner poly(S_{50}-*r*-$NBD2_{50}$) Fresnel lenses (D = 0.7 mm) were also readily fabricated using standard polishing methods with sandpaper and silica-based polishing compounds. Similarly, a freestanding 0.7-mm thick poly(S_{70}-*r*-$NBD2_{30}$) and poly(S_{50}-*r*-DIB_{50}) Fresnel lenses was directly cast as control imaging references, since these materials were too brittle, or soft to survive standard polishing methods. Freestanding *CHIPs* Fresnel lenses thinner than 0.7 mm were not able to be fabricated from these casting methods. Masked LWIR imaging conducted with the freestanding Fresnel lenses further demonstrates the importance of the material thermomechanical properties and fabrication processability, that were not as clearly evident for thin film NaCl-supported Fresnel lens experiments. The highest quality imaging was observed for poly(S_{50}-*r*-$NBD2_{50}$) Fresnel lenses which exhibited optimal imaging conditions at higher temperature ranges (T = 200–60 °C) in comparison to supported thin film Fresnel lenses (see Figure 3), where the thinner freestanding Fresnel lens (D = 0.7 mm) was able to resolve the UA-IR target at T = 60 °C, in comparison to the 1-mm thick Fresnel lens that could only be imaged above T = 100 °C (**Figure 4**a,b).

Masked LWIR imaging with the freestanding poly(S_{70}-*r*-$NBD2_{30}$) Fresnel lens exhibited similar viable temperature ranges as for the poly(S_{50}-*r*-$NBD2_{50}$) Fresnel lenses (T = 200–60 °C), but with reduced resolution of the UA-IR target; we note however, that while the resolution is definitely reduced the maximum brightness is increased. This is presumably due to the fact that the poly(S_{70}-*r*-$NBD2_{30}$) has reduced LWIR absorption compared to poly(S_{50}-*r*-$NBD2_{50}$), so more light gets through, but the increased scattering negatively impacts the resolution; this is more evident in the freestanding films because of the increased film thickness compared to the NaCl substrate-supported case. The poly(S_{50}-*r*-DIB_{50}) freestanding Fresnel lens (thickness = 0.7 mm) exhibited poor imaging quality of the UA-IR target even at high temperature (T = 200 °C), where the low T_g of freestanding poly(S_{70}-*r*-DIB_{30}) Fresnel lens (thickness = 0.7 mm) resulted in reflow within hours under ambient conditions after initial molding of the Fresnel lens shape, which, in addition to the intrinsically low LWIR transmission, rendered this useless as an IR plastic optic.

To further support these masked LWIR imaging experiments, direct black body LWIR imaging of a metallic aluminum target in the shape of a butterfly was conducted with these freestanding *CHIPs* Fresnel lenses after taking the heated metallic butterfly

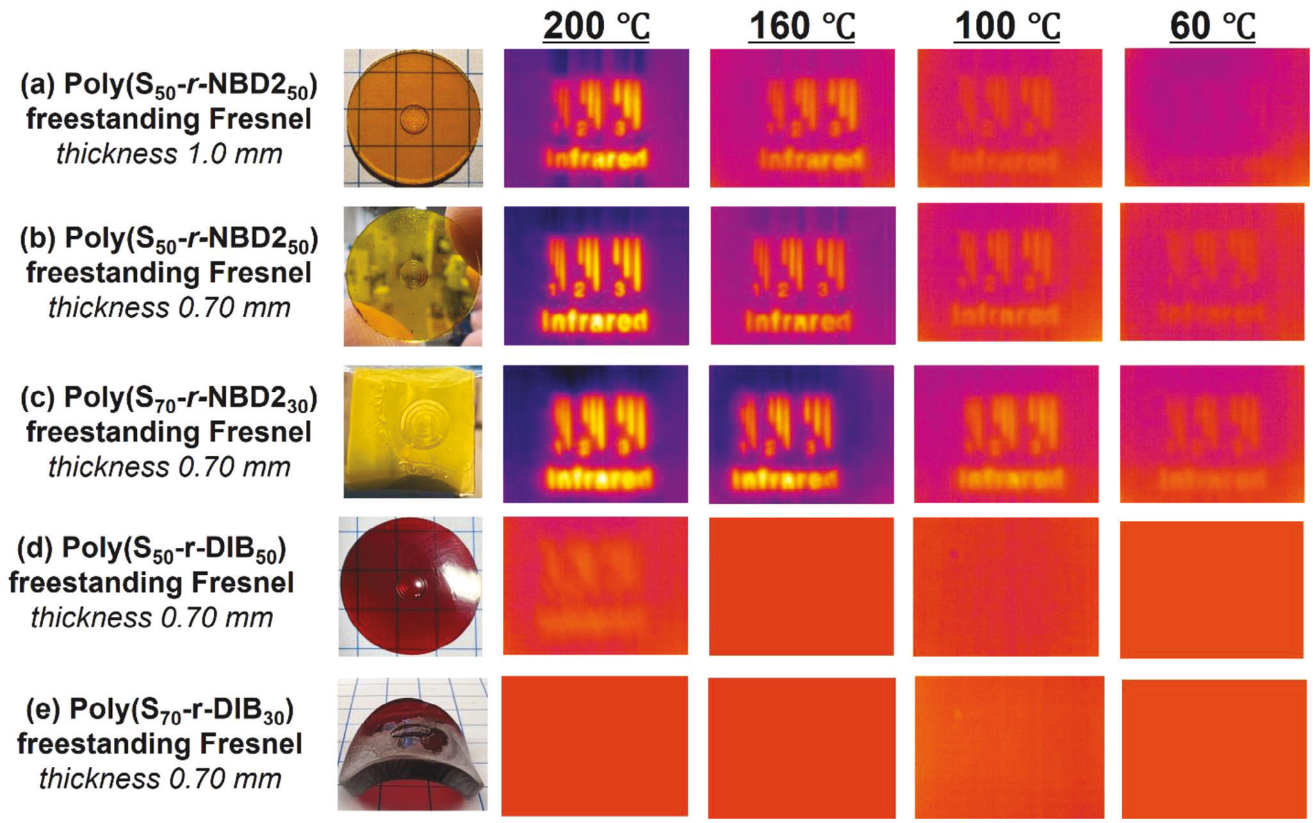

Figure 4. Masked LWIR imaging experiments conducted with UA-IR target and labscale imaging system from Figure 2 from $T = 200$–60 °C for freestanding: a) poly(S_{50}-*r*-$NBD2_{50}$) Fresnel lens (1-mm thickness), b) poly(S_{50}-*r*-$NBD2_{50}$) Fresnel lens (0.7-mm thickness), c) poly(S_{70}-*r*-$NBD2_{30}$) Fresnel lens (0.7-mm thickness), d) poly(S_{50}-*r*-DIB_{50}) Fresnel lens (0.7-mm thickness), and e) poly(S_{70}-*r*-DIB_{30}) Fresnel lens (0.7 mm thickness).

and capturing images at T = 100 °C and 50 °C which were found to be optimal temperatures for the AR-coated Ge plano-convex reference lens. As shown in **Figure 5**a, LWIR imaging of the butterfly subject afforded well-resolved images at both temperatures using the Ge reference lens, with the freestanding poly(S_{50}-*r*-$NBD2_{50}$) Fresnel lens afforded well-resolved images at T = 100 °C and reduced contrast, resolvable images at T = 50 °C (Figure 5b). LWIR imaging of the butterfly subject with the freestanding poly(S_{70}-*r*-$NBD2_{30}$) Fresnel lens exhibited reduced resolution at T = 100 °C in comparison to the freestanding poly(S_{50}-*r*-$NBD2_{50}$) Fresnel lens and was difficult to resolve at T = 50 °C, although with slightly enhanced brightness relative to the freestanding poly(S_{50}-*r*-$NBD2_{50}$) Fresnel lens at this temperature (Figure 5c) due to the factors discussed above.

The collective findings from both masked and black body LWIR imaging with freestanding *CHIPs* Fresnel lenses both validated the observations from supported thin film Fresnel lens experiments, while also revealing the importance of making freestanding plastic optics. Hence, while casting thicker freestanding Fresnel lenses of poly(S-*r*-NBD2) and poly(S-*r*-DIB) resulted in less optimal LWIR imaging conditions versus the supported the thin film Fresnel lenses, these bulk-free optic forms revealed which sulfur copolymer possessed the appropriate synergy of thermomechanical and optical properties, coupled with processability to fabricate viable IR plastic optic lenses. As alluded to in our prior work, new candidate optical polymers for IR optics should target achieving the thermomechanical properties and moldability of poly(methyl methacrylate) (PMMA, i.e., plexiglass) for fabrication of viable plastic optical elements.

3. Conclusion

We have demonstrated for the first time a facile fabrication process to produce IR plastic optics with *CHIPs* materials, specifically both supported and freestanding Fresnel lenses for LWIR thermal imaging. Furthermore, we have described the first complete methodology/system to fabricate and test new IR plastic optics *in operando* for LWIR imaging evaluation, where the effect of sulfur copolymer composition, lens format (supported vs freestanding) and imaging conditions (e.g., temperature effects) can be definitively determined. This study highlights the benefits of the *CHIPs* material, poly(S-*r*-NBD2), which exhibits a favorable ensemble of optical/thermomechanical properties, moldability, and low cost for fabrication of IR plastic optics, in which we demonstrate ambient, room temperature LWIR imaging with a LWIR designed refractive *CHIPs* lens for the first time. These collective findings also reveal the difficulties of extrapolating IR plastic optic performance based solely on sulfur content and IR spectroscopic transmittance of thin sulfur copolymer films. While the LWIR transparency of *CHIPs* materials needs to be improved to compete with existing state-of-the-art inorganic materials, the manufacturability of plastic optics based on *CHIPs* points to the

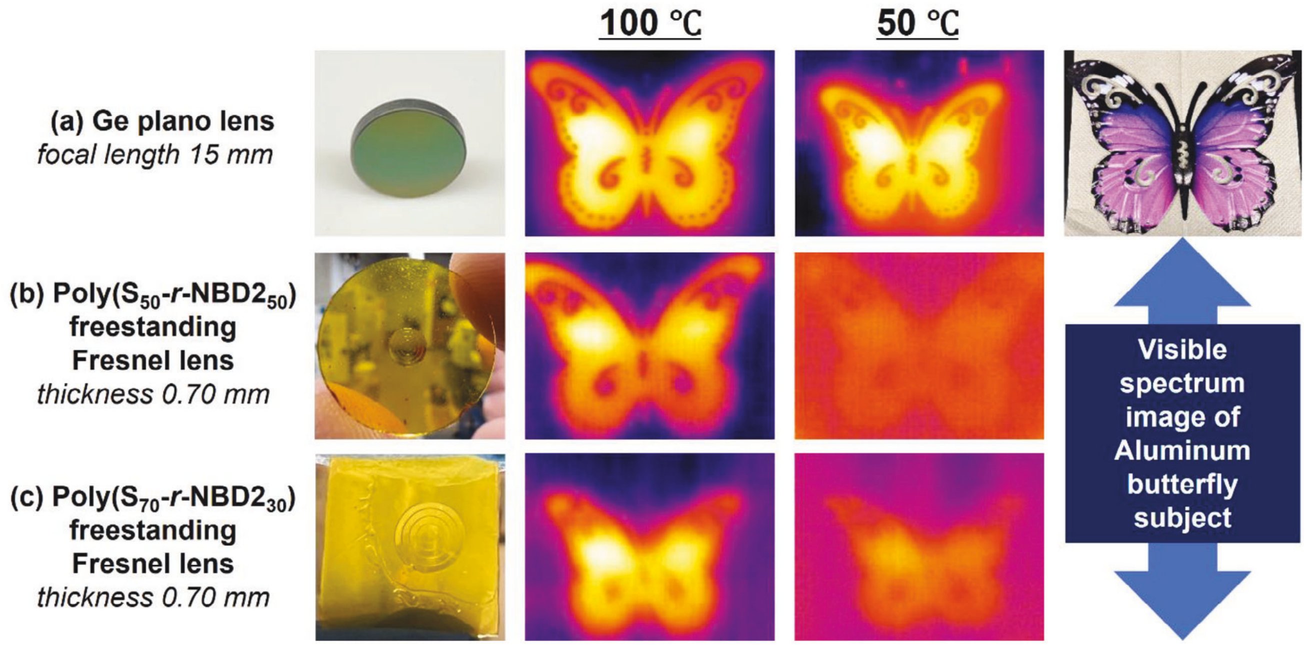

Figure 5. LWIR imaging experiments conducted with heated metallic butterfly $T = 100$ and 50 °C for freestanding: a) 15 mm focal length plano-convex Ge lens; b) poly(S_{50}-*r*-$NBD2_{50}$) Fresnel lens (0.7 mm thickness); and c) poly(S_{70}-*r*-$NBD2_{30}$) Fresnel lens (0.7 mm thickness).

value of this newly developing area of polymer science for IR optics & photonics.

Supporting Information

Supporting Information is available from the Wiley Online Library or from the author.

Acknowledgements

J.M. and T.L. contributed equally to this work. The authors gratefully acknowledge the National Science Foundation (PFI-RP 1940942, MRI-1920234), the Air Force Research Laboratories (FA8650-16-D-5404), MOBASE, Hyundai Motor Company, the RII Research Advancement Grant program from the University of Arizona, the Arizona Technology and Research Initiative Fund (A.R.S.§15-1648), and the National Science Foundation and the Air Force Research Laboratory through DMREF-2118578 for supporting this work. Gerald Uyeno and Raytheon Missiles Systems are gratefully acknowledged for helpful discussions and consultation on IR imaging system design.

Conflict of Interest

R.A. Norwood is an owner and officer of Norcon Technologies Holding Inc. with which a financial conflict of interest exists.

Data Availability Statement

The data that support the findings of this study are available in the supplementary material of this article.

Keywords

Fresnel lenses, infrared imaging, inverse vulcanization, optical polymers, plastic optics

Received: August 14, 2023
Revised: October 17, 2023
Published online:

[1] M. Vollmer, K.-P. Möllmann, *Infrared Thermal Imaging: Fundamentals, Research and Applications*, **2017**.

[2] T. S. Kleine, R. S. Glass, D. L. Lichtenberger, M. E. Mackay, K. Char, R. A. Norwood, J. Pyun, *ACS Macro Lett.* **2020**, *9*, 245.

[3] D. R. Rhiger, in *Semiconductors and Semimetals*, (Eds.: S. D. Gunapala, D. R. Rhiger, C. Jagadish), Elsevier, SanDiego, CA, USA **2011**, *Vol. 84*, pp. 303–331.

[4] N. A. Kulakova, A. R. Nasyrov, I. M. Nesmelova, *J. Opt. Technol.* **2010**, *77*, 324.

[5] a) J. J. Griebel, S. Namnabat, E. T. Kim, R. Himmelhuber, D. H. Moronta, W. J. Chung, A. G. Simmonds, K.-J. Kim, J. Van Der Laan, N. A. Nguyen, E. L. Dereniak, M. E. Mackay, K. Char, R. S. Glass, R. A. Norwood, J. Pyun, *Adv. Mater.* **2014**, *26*, 3014; b) J. J. Griebel, N. A. Nguyen, S. Namnabat, L. E. Anderson, R. S. Glass, R. A. Norwood, M. E. Mackay, K. Char, J. Pyun, *ACS Macro Lett.* **2015**, *4*, 862; c) T. S. Kleine, N. A. Nguyen, L. E. Anderson, S. Namnabat, E. A. Lavilla, S. A. Showghi, P. T. Dirlam, C. B. Arrington, M. S. Manchester, J. Schwiegerling, R. S. Glass, K. Char, R. A. Norwood, M. E. Mackay, J. Pyun, *ACS Macro Lett.* **2016**, *5*, 1152; d) L. E. Anderson, T. S. Kleine, Y. Zhang, D. D. Phan, S. Namnabat, E. A. Lavilla, K. M. Konopka, L. Ruiz Diaz, M. S. Manchester, J. Schwiegerling, R. S. Glass, M. E. Mackay, K. Char, R. A. Norwood, J. Pyun, *ACS Macro Lett.* **2017**, *6*, 500; e) T. S. Kleine, T. Lee, K. J. Carothers, M. O. Hamilton, L. E. Anderson, L. Ruiz Diaz, N. P. Lyons, K. R. Coasey, W. O. Parker Jr, L. Borghi, M. E. Mackay, K. Char, R. S. Glass, D. L. Lichtenberger, R. A. Norwood, J. Pyun, *Angew. Chem., Int. Ed.* **2019**, *58*, 17656.

[6] S. Gazzo, G. Manfredi, R. Pötzsch, Q. Wei, M. Alloisio, B. Voit, D. Comoretto, *J. Polym. Sci., Part B: Polym. Phys.* **2016**, *54*, 73.

[7] a) D. A. Boyd, C. C. Baker, J. D. Myers, V. Q. Nguyen, G. A. Drake, C. C. Mcclain, F. H. Kung, S. R. Bowman, W. Kim, J. S. Sanghera, *Chem.*

Commun. **2017**, *53*, 259; b) D. A. Boyd, V. Q. Nguyen, C. C. Mcclain, F. H. Kung, C. C. Baker, J. D. Myers, M. P. Hunt, W. Kim, J. S. Sanghera, *ACS Macro Lett.* **2019**, *8*, 113.

[8] a) W. J. Chung, J. J. Griebel, E. T. Kim, H. Yoon, A. G. Simmonds, H. J. Ji, P. T. Dirlam, R. S. Glass, J. J. Wie, N. A. Nguyen, B. W. Guralnick, J. Park, Á. Somogyi, P. Theato, M. E. Mackay, Y.-E. Sung, K. Char, J. Pyun, *Nat. Chem.* **2013**, *5*, 518; b) J. J. Griebel, R. S. Glass, K. Char, J. Pyun, *Prog. Polym. Sci.* **2016**, *58*, 90; c) M. J. H. Worthington, R. L. Kucera, J. M. Chalker, *Green Chem.* **2017**, *19*, 2748; d) J. M. Chalker, M. J. H. Worthington, N. A. Lundquist, L. J. Esdaile, *Top. Curr. Chem.* **2019**, *377*, 16; e) Y. Zhang, R. S. Glass, K. Char, J. Pyun, *Polym. Chem.* **2019**, *10*, 4078; f) T. Lee, P. T. Dirlam, J. T. Njardarson, R. S. Glass, J. Pyun, *J. Am. Chem. Soc.* **2022**, *144*, 5.

[9] J. M. Lee, G. Y. Noh, B. G. Kim, Y. Yoo, W. J. Choi, D.-G. Kim, H. G. Yoon, Y. S. Kim, *ACS Macro Lett.* **2019**, *8*, 912.

[10] M. Lee, Y. Oh, J. Yu, S. G. Jang, H. Yeo, J.-J. Park, N.-H. You, *Nat. Commun.* **2023**, *14*, 2866.

[11] J. H. Hwang, S. H. Kim, W. Cho, W. Lee, S. Park, Y. S. Kim, J.-C. Lee, K. J. Lee, J. J. Wie, D.-G. Kim, *Adv. Opt. Mater.* **2023**, *11*, 2202432.

[12] S. J. Tonkin, L. N. Pham, J. R. Gascooke, M. R. Johnston, M. L. Coote, C. T. Gibson, J. M. Chalker, *Adv. Opt. Mater.* **2023**, *11*, 2300058.

[13] a) T. S. Kleine, L. R. Diaz, K. M. Konopka, L. E. Anderson, N. G. Pavlopolous, N. P. Lyons, E. T. Kim, Y. Kim, R. S. Glass, K. Char, R. A. Norwood, J. Pyun, *ACS Macro Lett.* **2018**, *7*, 875; b) C. Tavella, P. Lova, M. Marsotto, G. Luciano, M. Patrini, P. Stagnaro, D. Comoretto, *Crystals* **2020**, *10*, 154.

[14] A. Nishant, K.-J. Kim, S. A. Showghi, R. Himmelhuber, T. S. Kleine, T. Lee, J. Pyun, R. A. Norwood, *Adv. Opt. Mater.* **2022**, *10*, 2200176.

[15] W. Cho, J. Hwang, S. Y. Lee, J. Park, N. Han, C. H. Lee, S.-W. Kang, A. Urbas, J. O. Kim, Z. Ku, J. J. Wie, *Adv. Mater.* **2023**, *35*, 2209377.

[16] M. Meem, S. Banerji, A. Majumder, F. G. Vasquez, B. Sensale-Rodriguez, R. Menon, *Proc. Natl. Acad. Sci. USA* **2019**, *116*, 21375.

[17] A. R. A. Manaf, T. Sugiyama, J. Yan, *Opt. Express* **2017**, *25*, 1202.

[18] a) M. Sussman, *Am. J. Phys.* **1960**, *28*, 394; b) M. Young, *J. Opt. Soc. Am.* **1972**, *62*, 972; c) J. Egger, *Some Advantages And Limitations*, SPIE, US **1979**, *Vol. 0193*.

[19] a) J. Engelberg, U. Levy, *Nat. Commun.* **2020**, *11*; b) M. K. Chen, Y. Wu, L. Feng, Q. Fan, M. Lu, T. Xu, D. P. Tsai, *Adv. Opt. Mater.* **2021**, *9*, 2001414.

[20] G. Bradburn, *Design and Manufacture of High Quality Plastic Infrared Fresnel Lenses*, SPIE, Cannes, France **1986**.

[21] T. Milster, in *Handbook of Optics*, (Ed: M. Bass), McGraw Hill, New York **1995**, Volume *II*.